Check for updates

Received: 18 September 2024 | Revised: 9 December 2024 | Accepted: 3 January 2025

IET Networks

DOI: 10.1049/ntw2.12143

The Institution of Engineering and Technology WILEY

ORIGINAL RESEARCH

An improved affinity propagation method for maximising system sum rate and minimising interference for 3D multi-UAV placement in disaster area

Nooshin Boroumand Jazi | **Farhad Faghani** | **Mahmoud Daneshvar Farzanegan**

Department of Electrical Engineering, Najafabad Branch, Islamic Azad University, Najafabad, Iran

Correspondence
Farhad Faghani.
Email: farhad.faghani@gmail.com

Abstract

In emergencies where several ground base stations (GBS) are no longer available, mobile base stations based on unmanned aerial vehicles (UAVs) can efficiently resolve coverage issues in remote areas due to their cost-effectiveness and versatility. Natural disasters, such as a deluge, cause damage to the terrestrial wireless infrastructure. The main challenge in these systems is to determine the optimal 3D placement of UAVs to meet the dynamic demand of users and minimise interference. Various mathematical frameworks and efficient algorithms are suggested for designing, optimising, and deploying UAV-based communication systems. This paper investigates the challenges of 3D UAV placement through machine learning (ML) and enhanced affinity propagation (EAP). Lastly, the simulation results indicate that the proposed approach improves the system sum rate, interference, and coverage performance compared to DBSCAN, k-means, and k-means++ methods. Therefore, this paper identifies UAVs' most effective 3D placement, including minimising the number of UAVs, maximising the number of covered users, and maximising the system sum rate for an arbitrary distribution of users in the disaster area. Additionally, this paper addresses the issue of interference minimisation.

KEYWORDS

5G mobile communication, data analysis, unsupervised learning

1 | INTRODUCTION

Unmanned aerial vehicles (UAVs) can assist the terrestrial GBS network in providing high data rate services whenever space and time are necessary. In contrast to terrestrial wireless networks, UAV networks possess numerous unique attributes, including highly dynamic network topologies, orbits, and flight trajectories. To extend the duration of flights, due to the energy source's limitations, it is necessary to incorporate low-energy design elements into airborne systems, such as path planning [1] and resource allocation [2]. In IoT networks, unmanned aerial vehicles (UAVs) can operate as stationary aerial base stations for IoT communications or act as mobile aggregators to collect data from IoT devices and transmit information to them. The integration of numerous sensors through IoT and machine-to-machine (M2M) communications is crucial for developing future applications, such as smart factories, smart farms, and smart cities [3, 4].

Furthermore, 6G technology is expected to provide a comprehensive framework for connected devices and automation systems, including self-driving cars and UAVs [5]. UAVs are increasingly regarded as vital components of these networks, as they enhance communication and computing capabilities at the devices' locations. Consequently, mobile edge computing services provided by UAVs can play a significant role in addressing the data processing needs of IIoT devices, effectively managing challenges related to computational offloading and latency [6].

To achieve optimal or near-optimal performance, one of the primary challenges of designing UAV-based communication systems is determining the appropriate horizontal and vertical position of UAVs and the path of movement of UAVs

This is an open access article under the terms of the Creative Commons Attribution License, which permits use, distribution and reproduction in any medium, provided the original work is properly cited.

© 2025 The Author(s). *IET Networks* published by John Wiley & Sons Ltd on behalf of The Institution of Engineering and Technology.

relative to other ground or flying objects [7]. Temporary coverage issues in remote areas or when terrestrial wireless infrastructure is damaged by a natural calamity, such as an earthquake or flood, can also be addressed by UAVs due to their rapid deployment in these areas. The 3D placement of UAVs is one of the most fundamental issues in UAV-based wireless communication. This paper examines UAVs' efficiency and optimal 3D deployment in emergency scenarios, considering network objectives such as enhancing network coverage, capacity, and system limitations. To delve into the research topic, we will concisely review the current literature regarding the optimal deployment of unmanned devices as aerial BSs in wireless networks.

In reference [8], the joint optimisation of placement and power allocation of multiple UAVs concerning ground users in an unknown area was performed. Game theory was employed to formulate the optimisation problem. Then, a robust and distributed learning algorithm is proposed to guide multiple UAV flight schedules to maximise the total rate for all ground users under specific flight areas and power constraints.

The authors in reference [9] proposed the decentralised optimisation of multiple UAV paths in real-time sensing applications using the Q-learning method, which was examined. An orthogonal frequency-division multiple access (OFDMA) single-cell UAV network was considered, where the UAVs transmit sensor data to a ground base station (BS) through orthogonal sub-channels to prevent mutual interference. The locations of the ground base station and the UAVs are specified with 3D coordinates. The authors in reference [10] investigated 3D UAV placement that maximises the number of covered users with different quality of service (QoS) requirements using minimum power. In this paper, the problem is modelled as a multiple concentric circles location problem to maximise the number of covered users. Then, the UAV deployment problem is separated into vertical and horizontal dimensions, and after some mathematical operations, an improved multi-population genetic algorithm (MPGA) is proposed. The authors in reference [11] minimise the total transmission power of users while satisfying some QoS constraints. Therefore, the performance of two proposed approaches for joint communication and positioning based on genetic algorithm (GA) and particle swarm optimisation (PSO) is investigated, and it is shown that both solutions improve user satisfaction with the provided data rate compared to the competitive approach. The results show that whereas PSO is less complex than GA, GA requires a small number of active UAVs to provide services to users. In reference [12], a multi-UAV system is considered where mobile base stations installed on the UAV serve the users on the ground. An iterative approach using block gradient descent is used to jointly optimise user timing, UAV trajectories, and transmission power to maximise throughput over all users. Subsequently, an innovative technique for initial path prediction was developed using a k-means clustering algorithm to divide users into subgroups and a genetic algorithm to initialise the shortest flight paths within clusters. In reference [13], k-means clustering is used for two-dimensional localisation between UAVs and users. A particle swarm optimisation (PSO)-based approach is proposed to maximise spectral efficiency while considering co-channel interference from other UAVs to determine the optimal altitude, ensuring the minimum required quality of service (QoS). The authors in reference [14] minimised the number and delay in UAV deployment which was examined. To this end, the minimum number of UAVs required to cover the disaster area was first determined using the k-means clustering algorithm, considering users' bandwidth constraints and determining the UAVs' two-dimensional coordinates. Then, a rapid UAV deployment algorithm was proposed to minimise the delay in UAV deployment. In reference [15], an optimal UAV deployment algorithm is proposed by considering the priority of ground nodes in various wireless communication environments. Solving the mixed integer second-order cone programming (MISOCP) problem finds the optimal UAV position. The authors in reference [16] proposed the k-means and a 3D UAV power allocation algorithm by Q-learning to maximise system capacity. In other words, a k-means algorithm is adopted to optimise horizontal positions and Q-learning to optimise power allocation.

Accordingly, the authors in reference [17] investigate the joint design of the 3D placement and power control for sum-rate maximisation. They decoupled the optimisation problem into two sub-problems: (i) 3D placement and user association and (ii) sum-rate maximisation. To solve the problem, they propose a heuristic algorithm to determine the minimum required UAVs. Then, an iteration algorithm is used to optimise the UAV 3D placement and user association. The authors in reference [18] presented an optimisation study to improve the lifespan of UAV-assisted cluster-based wireless sensor networks (WSNs) deployed in a 3D environment. This study is based on two algorithms: (1) particle swarm optimisation (PSO) for clustering problems in the WSN and (2) genetic algorithm (GA) for UAV placement to maximise the lifetime. The authors in reference [19] present a systematic mapping study on 3D placement in UAV-enabled communication systems. Heuristic algorithms prevail as the solution strategy. They focus on optimising data rate and throughput. Table 1 includes research related to placement in UAV-based communication networks.

As observed, there is a research gap regarding investigating UAV communications in emergency or disaster areas, which is worth studying to improve wireless services further. Additionally, the solutions used either employ mathematical modelling methods or, in most cases, reinforcement learning algorithms in machine learning methods. Reinforcement learning methods face numerous challenges, such as the need to implement and design a reward function, a significant demand for processing power, the difficulty in generalising different algorithms to environments, complex mathematical foundations, and the difficulty of implementation. In addition, game theory often relies on static strategies and without big data. Therefore, the proposed EAP algorithm can improve over time through learning from data and can be more dynamic, whereas game theory often relies on static methods. Because the data is significant

20474962, 2025, 1, Downloaded from https://ietresearch.onlinelibrary.wiley.com/doi/10.1049/ntw2.12143 by Readcube (Labtiva Inc.), Wiley Online Library on [10/03/2025]. See the Terms and Conditions (https://onlinelibrary.wiley.com/terms-and-conditions) on Wiley Online Library for rules of use; OA articles are governed by the applicable Creative Commons License

TABLE 1 Placement issues in UAV-based networks.

Reference	Placement target	Problem-solving method	Sum rate	User distribution	Interference	GBS Coexistence
Reference [8]	Sum rate	Game theory	Yes	Uniform	Yes	No
Reference [9]	Data transmission	Q-learning	No	-	Yes	No
Reference [10]	QoS	MPGA	No	Uniform	No	No
Reference [11]	Total power	PSO	No	Uniform	No	No
Reference [12]	Throughput	kmeans	No	Random	Yes	No
Reference [13]	QoS	PSO, k-means	No	PPP	Yes	No
Reference [14]	Coverage	k-means	No	Random	No	No
Reference [15]	Coverage	MISOCP	No	PPP	No	No
Reference [16]	Capacity	Q-learning	No	Uniform	Yes	No
Reference [17]	Sum rate	Heuristic	No	Random	Yes	No
Reference [18]	System lifetime	PSO, GA	No	Random	No	No
Reference [19]	Throughput	Heuristic	No	-	Yes	No
This paper	Sum rate	EAP	Yes	Arbitrary	Yes	Yes

in this problem and the environment is dynamic, the proposed EAP algorithm is more efficient and can adapt to changing data and environments.

This paper proposes a data-driven 3D placement for multiple UAVs in emergency or disaster areas. We focus on high-density scenarios with heterogeneous UE distributions. The proposed deployment method should automatically determine the number, location, altitude, and coverage of appropriate UAVs. This issue will address optimising the system sum rate and minimising interference. For this purpose, propagation models will be explained in Section 2. Then, in Section 3, the proposed 3D placement algorithm will be presented. In Section 4, the simulation results of the proposed algorithm will be evaluated, and finally, in Section 5, the conclusion will be stated.

2 | SYSTEM MODEL

A cellular system is considered where one or more ground base stations (GBS) are inactive due to congestion or infrastructure failure. Therefore, a network of UAVs is deployed to maintain connectivity for ground terminals. An urban area with a specific number of users is considered. The goal is to find the minimum number of UAVs and their 3D locations to provide services to users in that area. A UAV-assisted cellular system consisting of one GBS and a set of UAVs, $u = \{U_1, U_2, \ldots, U_k\}$, is considered. In an urban scenario, K is the maximum number of available UAVs. With the help of UAV, the cellular system provides services to a set of UEs, $E = \{u_1, u_2, \ldots, u_N\}$, and the total number of UEs is $|E| = N$. Radio propagation models for downlink transmissions include three modes, which will be discussed in the following sections.

2.1 | GBS-to-UAV propagation model

In the considered system model, the GBS uses directional mmWave antennas to transmit signals to the UAV. UAVs fly at relatively high altitudes, so the GBS-to-UAV channel would be the most straightforward path loss model using LoS links between the GBS and the UAV that propagate in open space; the average path loss in dB of the 28 GHz mmWave signal is presented in reference [20].

$$L_{j,G}^{bk} = 61.4 + 20\log_2\left(d_{j,G}\right) \tag{1}$$

where $d_{j,G}$ is the distance between the GBS and Uj and $j = 1, 2, \ldots, k$ is in metres.

$$P_j^R = P_G^{mmWave}\, g_G^T g_j^R \left(\frac{c}{4\pi d_{j,G} f_c^{mmWave}}\right)^2 \tag{2}$$

where P_G^{mmWave} is the constant transmission power of the mmWave antenna, g_G^T is the gain of the GBS transmitting antenna, g_j^R is the receiving gain of the Uj antenna, c is the speed of light, f_c^{mmWave} is the carrier frequency used in the backhaul link. According to Equation (1), the received signal-to-noise ratio (SNR) in a UAV is as follows:

$$\gamma_{j,G} = \frac{P_G^{mmWave}\left(10^{L_{j,G}^{bk}/10}\right)^{-1}}{B_{j,G}^{mmWave} N_0} > \gamma_{th}^{bk} \tag{3}$$

where $B_{j,G}^{mmWave}$ is the allocated bandwidth (in Hz) of the mmWave backhaul link for UAV, Uj, and N_0 is thermal noise power spectrum density and γ_{th}^{bk} is a certain threshold of the mmWave backhaul transmission. According to Equation (3)

20474962, 2025, 1, Downloaded from https://ietresearch.onlinelibrary.wiley.com/doi/10.1049/mw2.12143 by Readcube (Labtiva Inc.), Wiley Online Library on [10/03/2025]. See the Terms and Conditions (https://onlinelibrary.wiley.com/terms-and-conditions) on Wiley Online Library for rules of use; OA articles are governed by the applicable Creative Commons License

and Shannon's theorem, the backhaul capacity of a UAV, Uj, can be shown as follows:

$$\hat{C}_j = B_{j,G}^{mmWave} \log_2\left(1 + \gamma_{j,G}\right) \quad (4)$$

2.2 | UAV-to-UE propagation model

The second propagation model is used for the downlink transmission from a UAV to a UE. The authors in reference [21] modelled the air-to-ground (ATG) channel with derivations of the probabilities of LoS (line of sight) and NLoS (non-line of sight) signals, and now their proposed channel model is widely used in UAV communications. Such a radio propagation model is known as an air-to-ground propagation channel. It is typically modelled by considering LoS and NLoS signals separately, along with their respective probabilities. The effect of fading can be ignored because it only accounts for a small percentage [22]. The average ATG channel model between a UAV and a ground user is denoted as $\overline{L_{i,j}}$, where $\overline{L_{i,j}} = P_{\text{LoS}} \times \text{PL}_{\text{LoS}} + P_{\text{NLoS}} \times \text{PL}_{\text{NLoS}}$. Where PL_{LoS} and PL_{NLoS} indicate the path loss of different signal groups in the air-to-ground link and also the probability of $P_{\text{NLOS}} = 1 - P_{\text{LOS}}$. According to reference [21], $\overline{L_{i,j}}$ was measured.

$$\overline{L_{i,j}} = \frac{A}{1 + C\exp(-D[\theta - C])} + 10\log\left(h^2 + r^2\right) + B \quad (5)$$

where $A = \eta_{\text{LoS}} - \eta_{\text{NLoS}}$, η_{LoS} and η_{NLoS} are the average additional losses for LoS and NLoS in dB, $B = 20\log f_c + 20\log 4\pi/_c + \eta_{\text{NLoS}}$, f_c is the carrier frequency of the fronthaul link. C and D are constants that depend on the environment (rural, urban, dense urban or other), and θ is the elevation angle. Clearly, $\theta = \frac{180}{\pi}\sin^{-1}\left(\frac{h_i}{d_i(x,y)}\right)$, $d_i(x,y) = \sqrt{(x - x_i)^2 + (y - y_i)^2 + h_i^2}$.

The parameter values are shown in Table 2:

$P_{i,j}$, is the minimum transmission power required to send a signal from the UAV to a UE, if the received signal-to-interference-plus-noise ratio (SINR) in a UE is greater than the threshold value γ_{th}, the transmission is successful. Therefore, the SINR for each UE associated with the UAV U_j is equal to the following equation:

$$\gamma_{i,j} = \frac{P_{i,j}\left(10^{\overline{L_{i,j}}/10}\right)^{-1}}{I_G + I_{u\setminus\{U_j\}} + B_{i,j}N_0} > \gamma_{th} \quad (6)$$

where I_G is the received interference power from the GBS and $I_{u\setminus\{U_j\}} = \sum_{j'=1}^{k} P_{i,j'}\left(10^{\overline{L_{i,j'}}/10}\right)^{-1}\psi_{j,j'}$ is the interference power of nearby UAVs. $\psi_{j,j'} = 1$ if u_i is located in the overlapping coverage area of UAV U_j and $U_{j'}$, and $U_{j'} \in u, \forall j' \neq j$ otherwise $\psi_{j,j'} = 0$. According to Shannon's theorem and Equation (6), the allocated data rate (in bps) of each u_i associated with U_j will be as follows:

$$c_{i,j} = B_{i,j}\log_2\left(1 + \gamma_{i,j}\right) \quad (7)$$

where $B_{i,j}$ is the allocated bandwidth (in Hz) of the wireless connection from the UAV to each u_i. The transmission power assigned to the desired u_i can be given by the following equation:

$$P_{i,j} = 10^{\overline{L_{i,j}}/10}\left(I_G + I_{u\setminus\{U_j\}} + B_{i,j}N_0\right)\left(2^{c_{i,j}/B_{i,j}} - 1\right) \quad (8)$$

Then, the total transmission power of the UAV to serve its associated u_i can be calculated as follows:

$$P_j = \sum_{i=1}^{N_j} P_{i,j} \quad (9)$$

where N_j is the number of UEs associated with each UAV. According to Equation (9), the data transmission rate of the UAV to serve its associated UEs:

$$C_j = \sum_{i=1}^{N_j} c_{i,j} \quad (10)$$

2.3 | GBS-to-UE propagation model

For the terrestrial wireless channel between points p_1 and p_2, a standard path loss power law $L_{p_1,p_2} = \|p_1 - p_2\|^{-\alpha}$ with path power loss $\alpha > 2$ is considered. All terrestrial broadcast signals are assumed to experience independent Rayleigh fading, and the GBS transmits with fixed power P_G for terrestrial communications. Therefore, the received power of each UE provided by the GBS is $P_G h r_{i,G}^{-\alpha}$, where $h \sim exp(1)$ is the Rayleigh fading and $r_{i,G}$ is the horizontal distance between the UE and the GBS. Because there are k UAVs in the considered

TABLE 2 Propagation parameters [23].

Environment	C	D	η_{LoS}	η_{NLoS}
Suburban	4.88	0.43	0.1	21
Urban	9.61	0.16	1	20
Dense urban	12.08	0.11	1.6	23
High-rise urban	27.23	0.08	2.3	34

20474962, 2025, 1, Downloaded from https://ietresearch.onlinelibrary.wiley.com/doi/10.1049/ntw2.12143 by Readcube (Labtiva Inc.), Wiley Online Library on [10/03/2025]. See the Terms and Conditions (https://onlinelibrary.wiley.com/terms-and-conditions) on Wiley Online Library for rules of use; OA articles are governed by the applicable Creative Commons License

system, the co-channel interference power experienced by a UE can be expressed as follows:

$$I_U = \sum_{j=1}^{k} P_j h r_{i,j}^{-\alpha} = \sum_{j=1}^{k} P_j \left(10^{\overline{L_{i,j}}/10}\right)^{-1} \tag{11}$$

where P_j is the transmission power of the UAV and $r_{i,j}$ is the distance of each UE to the UAV. The SINR statement for each user that can connect to the GBS is as follows:

$$\gamma_{i,G} = \frac{P_G h r_{i,G}^{-\alpha}}{I_U + B_{i,G} N_0} > \gamma_{th} \tag{12}$$

where $I_U = \sum_{\forall U_j \in u} P_j \left(10^{L_{h,r}/10}\right)^{-1}$ is the total interference power from other isolated UAVs and $B_{i,G}$ is the allocated bandwidth (in Hz) to the UE with the GBS. The achievable data rate (in bps) of a UE associated with the GBS can be calculated as follows:

$$c_{i,G} = B_{i,G} \log_2\left(1 + \gamma_{i,G}\right) \tag{13}$$

Thus, the potential transmission rate (in bps) of the GBS can be obtained.

$$C_G = \frac{\lambda_G}{\pi r_G^2} \overline{c_{i,G}} = \sum_{i=1}^{N_G} c_{i,G} \tag{14}$$

where r_G is the GBS coverage radius, λ_G is the UE density of the GBS service coverage, $\overline{c_{i,G}}$ is the average data rate of a UE associated with the GBS, and N_G is the number of UEs associated with the GBS.

3 | THE PROPOSED 3D PLACEMENT ALGORITHM

The decision-making problem for placing the 3D UAV can be defined as follows. The considered problem is to search for suitable location parameters $\left(x_j, y_j, h_j, r_j\right)$ of each UAV with a minimum number of k. $0 \le k \le K$, so that:

$$\max_{x_j, y_j, h_j, r_j} \sum_{i=1}^{N} c_{i,G}\delta_{i,G} + \sum_{j=1}^{k} \sum_{i=1}^{N} c_{i,j}\delta_{i,j} \tag{15}$$

$$s.t.\ \ r_j \le r_{\max}\left(h_j\right) \tag{16}$$

$$h_{\min} \le h_j \le h_{\max} \tag{17}$$

$$c_{i,j}\delta_{i,j} + c_{i,G}\delta_{i,G} \ge c_{\min}, i = 1, 2, \ldots, N$$

$$j = 1, 2, \ldots, k \tag{18}$$

$$\sum_{i=1}^{N} c_{i,G}\delta_{i,G} \le \hat{C}_G \tag{19}$$

$$\sum_{i=1}^{N} c_{i,j}\delta_{i,j} \le \hat{C}_j \quad j = 1, 2, \ldots, k \tag{20}$$

$$\sum_{i=1}^{N} \delta_{i,G} + \sum_{j=1}^{k} \sum_{i=1}^{N} \delta_{i,j} = N \tag{21}$$

where the two indicator functions $\delta_{i,G}$ and $\delta_{i,j}$ are defined as follows:

$$\delta_{i,j} = \begin{cases} 1, & if\ \gamma_{i,j} > \gamma_{th} \\ 0, & \text{otherwise} \end{cases}$$

$$\delta_{i,G} = 1 - \sum\nolimits_{j=1}^{k} \delta_{i,j} \tag{22}$$

In the considered problem Equation (15), the maximum coverage U_j, $r_{\max}\left(h_j\right)$ in Equation (16), and the relationship between the height and the maximum coverage of a UAV are discussed in reference [24]. In constraint Equation (17), the deployed height of each UAV depends on the constraints of local laws and the capability of the UAV. Additionally, in Equation (18), we consider the minimum data rate demands from the cellular operator aspect and define a parameter $c_{\min}$ for each UAV or GBS to guarantee the minimum data rate allocated to a UE within the constraints. Constraint Equation (19) guarantees that the total transmission rate of the downlink connection from the GBS and its associated UEs does not exceed the maximum data rate capability $\hat{C}_G$. Constraint Equation (20) is used so that the total transmission rate of the downlink from the UAV to its associated UEs does not exceed the maximum data rate allocated to the backhaul link in U_j. Constraint Equation (21) causes each UE to be associated with only one UAV or GBS at a time.

Next, a data-based location is proposed to improve the overall performance of the UAV-assisted cellular system, especially for unpredictable events or flash congestion with high-density distributed users.

In Equation (15), the system sum rate mainly depends on $N_j = \sum_{i=1}^{N} \delta_{i,j}$ and $N_G = 1 - \sum_{j=1}^{N} \delta_{i,j}$, which are determined by UAV positioning. The proposed approach uses the location information of UEs, UAVs and GBSs to provide an effective location of the UAV. The variable $L_G = \left(x_G, y_G\right)$ records the coordinates of the GBSs, an array L_E stores the location of the UEs, and an array L_U stores the location (coordinates) of the UAV. In the initialisation phase, the system calculates the received power of each UE from the GBS and $P_{i,G}^{R} = P_G h r_{i,G}^{-\alpha}$ in a set S_G, where $1 \le i \le N$ stores. GBS distances to all UEs are stored in a D_G set. Intuitively, the UAV is used to assist the GBS, and first, the initial communication between the GBS and each UE is established. Because the number and location of deployed UAVs are unknown at this stage, the interference power cannot be obtained. Instead, the initial connection between the GBS and each UE is determined by the condition $\gamma_{i,G} > \gamma_{th}$, where $\gamma_{i,G}$ is the SINR regardless

20474962, 2025, 1, Downloaded from https://ietresearch.onlinelibrary.wiley.com/doi/10.1049/ntw2.12143 by Readcube (Labtiva Inc.), Wiley Online Library on [10/03/2025]. See the Terms and Conditions (https://onlinelibrary.wiley.com/terms-and-conditions) on Wiley Online Library for rules of use; OA articles are governed by the applicable Creative Commons License

of interference. The number of UEs with SINR values higher than γ_{th} is represented as N_G^{temp}. In addition, according to Equations (13) and (18), the upper bound of N_G can be obtained as follows:

$$N_G^{\max} = B \log_2\left(1 + \gamma_{th}\right)/c_{min} \tag{23}$$

where $B_{i,G} = B/N_G$. Therefore, we select $N_G = \min\left(N_G^{\text{temp}}, N_G^{\max}\right)$ UEs with high SINR values associated with the GBS.

After the initial GBS communication, the system can determine the number of UAVs for clustering UEs using the enhanced affinity propagation algorithm. Density-based clustering is a method of clustering data based on the density of points in the data space. The DBSCAN (density-based spatial clustering of applications with noise) algorithm is one of the famous algorithms in this category, and it performs well in cases where the data has irregular shapes. Still, for enormous data sets, the calculations can be time consuming. Hierarchical clustering is another data clustering method that creates a hierarchical or tree structure of clusters. Unlike partitioning clustering methods (such as k-means), instead of creating a fixed set of clusters, it makes a tree structure that shows how the clusters are composed of or related to each other and is useful when the hierarchical structure of the data is of interest. Therefore, it is not suitable for data in this problem. Unlike traditional clustering algorithms such as k-means or hierarchical clustering, the AP algorithm does not need to determine the number of clusters in advance. The advantage of the AP algorithm is its ability to determine the number of clusters automatically based on the input data [25]. Instead of using a similarity (distance) matrix, this algorithm uses three matrices to find affinity: (a) similarity matrix, (b) responsibility matrix, and (c) accessibility matrix. In each step of this algorithm, the mentioned matrices are updated, and the updating process is repeated so that the changes do not exceed the tolerance limit set by the user. This algorithm is suitable for data that can have many clusters.

In the second step, each UE is associated with at least one UAV. Therefore, for each UE, $\gamma_{i,j}$ must be greater than the specified threshold γ_{th} so that each u_i can be associated with the UAV. Generally, the allocated data rate c_i and SINR $\gamma_{i,j}$ of u_i increase when the distance $r_{i,j}$ between u_i and U_j decreases. We consider a variation of the weighted assignment problem, the capacity clustering problem (CCP). CCP is an NP-complete decision problem. Given a set of N UEs and a set of k UAVs $k < N$, if $r_{i,j}$ is the horizontal distance between UE and UAV (cluster centre), then $c_{i,j}$ the allocated data rate from UE, $\hat{C}_j$ is the backhaul limit for the UAV, and then find k distinct subsets of UEs such that the total horizontal distance value of the selected UEs is minimal. Each subset can be assigned to a different UAV whose backhaul limit is less than the total horizontal distance of UEs, which is not in the subset. So,

$$\min \sum_{j=1}^{k} \sum_{i=1}^{N} r_{i,j}\delta_{i,j} \tag{24}$$

Note that $r_{i,j}$ in Equation (24) represents the cost function for clustering. A customised cost function can be substituted for $r_{i,j}$ to obtain a different clustering result. At this stage, the k-medoid clustering method is adopted in the proposed method. In k-medoids, the cluster centre is a real data point and can be easily interpreted. Therefore, it is less sensitive to outliers and provides more stable clustering.

After this step, the system receives the k-centre point of the generated clusters. Suppose the horizontal coverage of each UAV-to-ground mapping is considered an ideal circle, and each UAV is deployed directly at the centre point of each cluster. In that case, the horizontal coverage radius of each UAV is the horizontal distance from the centre point to the farthest UE of each cluster—however, a system with such positioning results in a large coverage area. If the coverage area of the overlapping area increases, the distance between different deployed UAVs is short. Such placement may lead to severe interference between UAVs. Most dissatisfied users are located in overlapping coverage areas. Therefore, reducing interference improves user satisfaction and ensures that most UEs achieve the minimum data rate [26].

The last task of this step is to judge whether the obtained candidate position is valid by checking the presence of dissatisfied UEs. If there are any unsatisfied UEs, the obtained candidate location is invalid, and the value of k may be too small to satisfy the UE demand in the considered scenario. Thus, the system performs the entire steps of this step repeatedly with $k = k + 1$ until the obtained candidate location is valid.

4 | RESULTS

The simulation framework leverages the power and flexibility of the Python programming language. Because of the unavailability of accurate data, we artificially generate sets of input spatial data with a non-uniform distribution over an area of 1200 square meters, which includes a varying number of UE locations [27]. The generated data accurately reflects the characteristics of the original data. We consider an urban scenario. The urban scenario and air-to-ground channel model provided by the authors in reference [5] $\left(c, d, \eta_{\text{LoS}}, \eta_{\text{NLoS}}\right) = (9.61, 0.16, 1, 20)$ are considered, and the maximum allowable path loss for the UAV-to-UE link $L_{h,r}^{\max} = 119\, dB$ is assumed. Other important simulation parameters and predefined constraints are presented in Table 3.

To compare the proposed method, namely the enhanced affinity propagation (EAP) algorithm, DBSCAN, k-means, and k-means++ approaches [28] are used in the simulation. The GBS is located at the coordinate (500, 700) in this scenario. In Figure 1, the blue triangle represents the GBS, the black crosses represent the UAVs, the tiny dots represent the UEs, and each circle represents the corresponding UAV coverage area. This method uses the enhanced affinity propagation (EAP) algorithm.

20474962, 2025, 1, Downloaded from https://ietresearch.onlinelibrary.wiley.com/doi/10.1049/ntw2.12143 by Readcube (Labtiva Inc.), Wiley Online Library on [10/03/2025]. See the Terms and Conditions (https://onlinelibrary.wiley.com/terms-and-conditions) on Wiley Online Library for rules of use; OA articles are governed by the applicable Creative Commons License

TABLE 3 Simulation parameters [27].

Parameter	Value	Parameter	Value	Parameter	Value
P_G	40 dBm	P_j	20 dBm	P_G^{mmWave}	30 dBm
α	6.5	$c_{\min}$	10^6 bps	N_0	−174 dBm/Hz
$h_{\min}$	20 m	f_c	2 GHz	f_c^{mmWave}	28 GHz
$h_{\max}$	400 m	B	20 MHz	B_j^{mmWave}	2000 MHz
γ_{th}	5 dB	γ_{th}^{mmWave}	30 dB		

The simulation results are as follows:

Figure 2 shows the optimal height of each UAV with $k = 27$ in the proposed method. Figure 3 shows the placement results using the DBSCAN, k-means, and k-means++ clustering algorithms.

Figure 3 shows the results of location for $N = 1300$ using the DBSCAN with $k = 52$, k-means with $k = 42$, and k-means++ with $k = 37$ clustering algorithms. Therefore, in the proposed method, placement can be optimised with fewer UAVs. Unlike

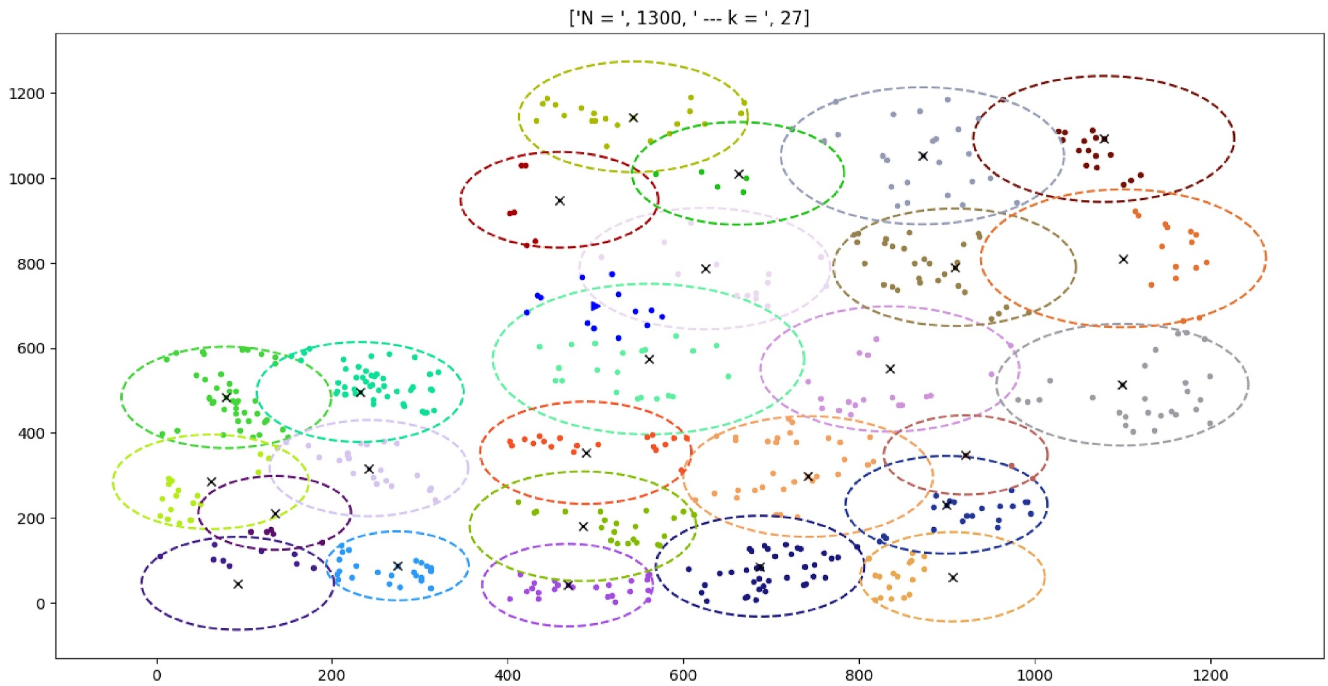

FIGURE 1 Placement results with $k = 27$, $N = 1300$.

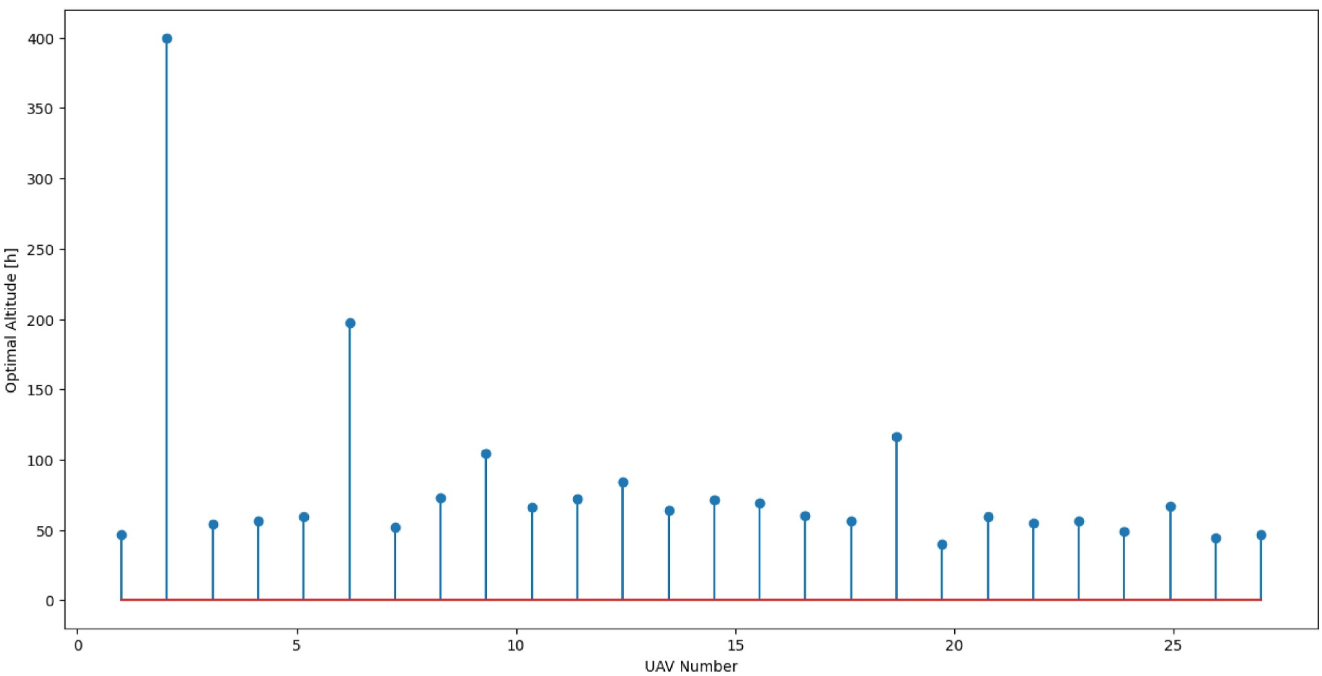

FIGURE 2 The optimal height of each UAV in the proposed method.

20474962, 2025, 1, Downloaded from https://ietresearch.onlinelibrary.wiley.com/doi/10.1049/ntw2.12143 by Readcube (Labtiva Inc.), Wiley Online Library on [10/03/2025]. See the Terms and Conditions (https://onlinelibrary.wiley.com/terms-and-conditions) on Wiley Online Library for rules of use; OA articles are governed by the applicable Creative Commons License

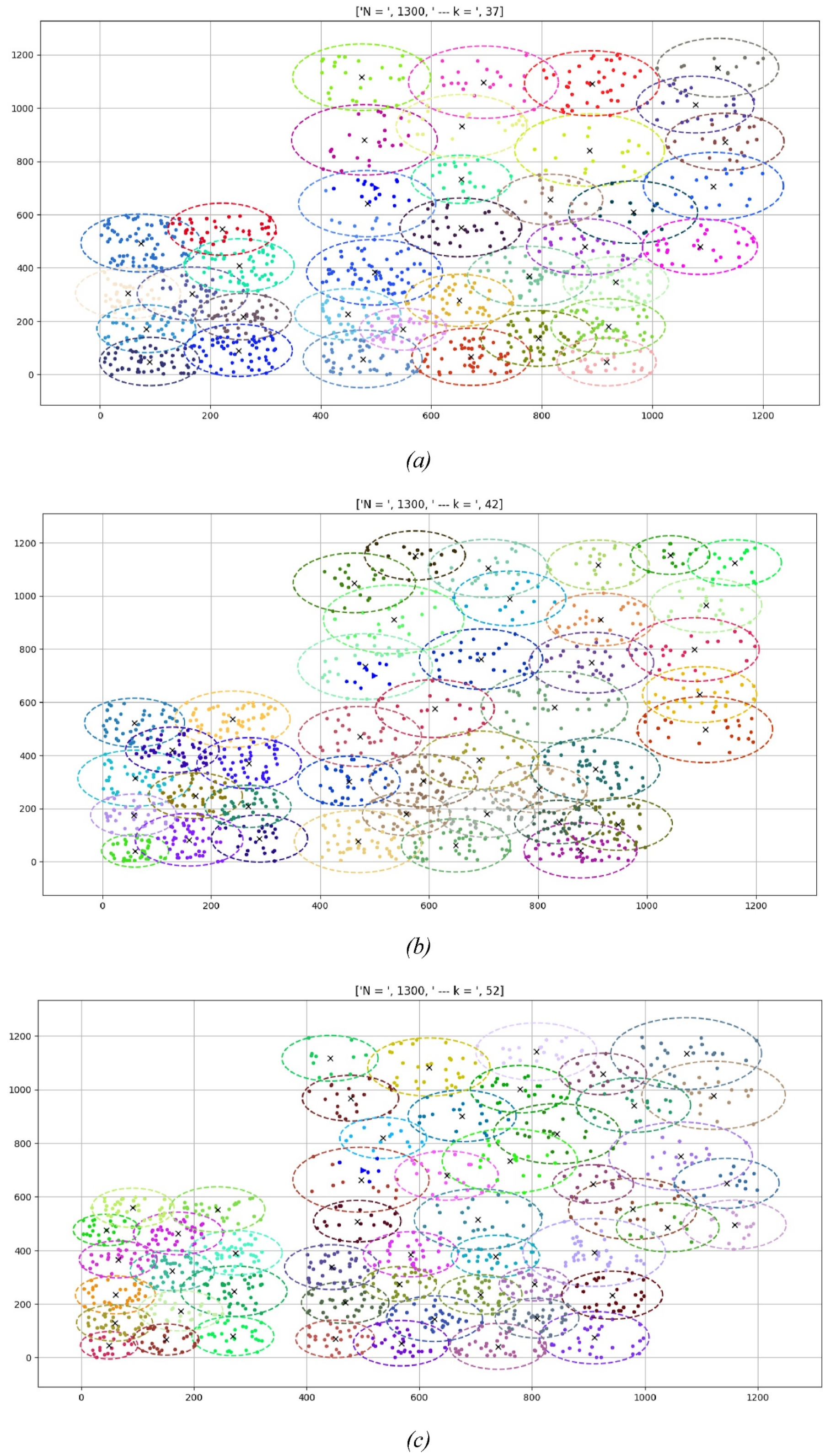

FIGURE 3 Placement results (a) k-means++ with $k = 37$, $N = 1300$, (b) k-means with $k = 42$, $N = 1300$, and (c) DBSCAN with $k = 52$, $N = 1300$.

the conventional approaches, which cannot determine the value of k by the algorithms themselves, the proposed method can automatically determine the value of k. For instance, in the k-means method, the algorithm starts from the initial value of $k = 28$ and reaches the value of $k = 42$, and the algorithm repeats every step, which takes a lot of calculation time. Consequently, the system can save significant computational costs (time and energy) when evaluating the impossible value of k.

In the following, we present an analysis of clustering metrics. Several metrics can be used to evaluate the quality of

20474962, 2025, 1, Downloaded from https://ietresearch.onlinelibrary.wiley.com/doi/10.1049/ntw2.12143 by Readcube (Labtiva Inc.), Wiley Online Library on [10/03/2025]. See the Terms and Conditions (https://onlinelibrary.wiley.com/terms-and-conditions) on Wiley Online Library for rules of use; OA articles are governed by the applicable Creative Commons License

TABLE 4 Definitions of metrics.

Metrics	Definition	Range
Silhouette score	It is calculated based on the difference between the intra-cluster distance and the closest distance to another cluster. A value closer to +1 indicates better clustering.	Between −1 and 1
Davies–Bouldin index	It is the ratio of the intra-cluster distance to the distance between clusters. A lower value in the Davis–Bouldin index indicates more effective clustering.	No upper bound, but lower values (ideally close to 0)
Calinski–Harabasz index	Measures the ratio of the distance between clusters to the distance within clusters. A higher value in this index indicates higher-quality clustering.	Does not have a strict upper bound.

TABLE 5 Comparison of clustering methods with different metrics.

Metrics	DBSCAN	*k*-means	*k*-means++	Proposed method
Silhouette score	−0.4383	−0.1733	0.3116	0.5529
Davies–Bouldin index	1.8788	1.7671	0.8439	0.1799
Calinski–Harabasz index	31.6746	37.9824	50.9581	68.5303

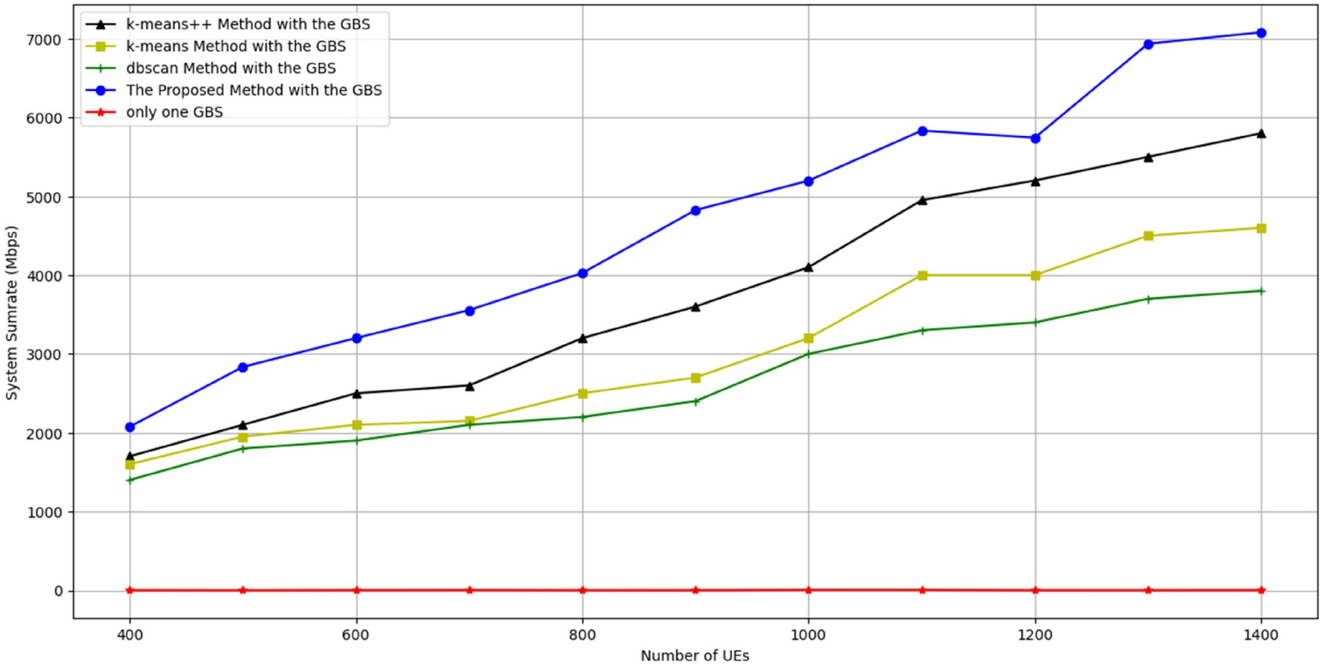

FIGURE 4 Comparing the system sum rate in the proposed method with GBS, the *k*-means++ method with GBS, the *k*-means method with GBS, the DBSCAN method with GBS, and only one GBS without UAVs.

the proposed clustering method, with the choice depending on the data type and clustering objective. Distance-based metrics assess clustering quality without requiring actual class labels. Because accurate class labels are unavailable (unsupervised clustering), the Silhouette, Davies–Bouldin, and Calinski–Harabasz indices are employed. Table 4 shows the definitions of these three metrics and their ranges [29].

Subsequently, the Silhouette score, Davies–Bouldin index, and Calinski–Harabasz index were computed for each clustering result to observe the performance metrics, shown in Table 5. Table 5 shows that the Silhouette score in the proposed method is 0.5529, indicating a good separation between clusters. The Silhouette score is greater than 0, indicating that the algorithm has effectively generated clusters and has not encountered overlap, and the interference problem is completely solved. On the other hand, when the Calinski–Harabasz score in the proposed method is 68.5303, it indicates relatively high cluster density and separation in that specific number of clusters, and there is significant differentiation between clusters, indicating a favourable clustering result. In addition, the Davies–Bouldin score of 0.1799 indicates excellent separation between the clusters. Therefore, the proposed method has better clustering than DBSCAN, *k*-means, and *k*-means++ methods in terms of the three metrics: the Silhouette score, Davies–Bouldin index, and Calinski–Harabasz index, and is more capable of solving the problem of interference.

Figure 4 compares the system sum rate in different methods despite the different UE numbers between 400 and 1400.

Figure 4 shows that deploying UAVs in the proposed method, compared to scenarios without UAVs and scenarios

20474962, 2025, 1, Downloaded from https://ietresearch.onlinelibrary.wiley.com/doi/10.1049/ntw2.12143 by Readcube (Labtiva Inc.), Wiley Online Library on [10/03/2025]. See the Terms and Conditions (https://onlinelibrary.wiley.com/terms-and-conditions) on Wiley Online Library for rules of use; OA articles are governed by the applicable Creative Commons License

with k-means, k-means++, and DBSCAN clustering algorithms, significantly increases the system sum rate.

5 | CONCLUSION AND FUTURE WORK

This paper investigates the optimal 3D placement of unmanned aerial vehicles (UAVs) with ground-based systems (GBSs) to provide services in emergency areas with variable population density. A novel 3D placement algorithm based on enhanced affinity propagation is presented in this regard. Unlike existing methods, the proposed algorithm can determine the optimal number, placement, and coverage of each UAV. Simulation results show that the proposed approach improves the system sum rate compared to the comparative methods DBSCAN, k-means, and k-means++, while effectively providing the minimum required data rate for each user (UE). In addition, the proposed algorithm significantly avoids the interference problem. These findings indicate the high efficiency of the proposed algorithm in optimising the placement of UAVs to provide emergency services in environments with variable population densities. Furthermore, future directions could include innovations in energy management, potentially involving techniques like dynamic power control, weather conditions, and prolonged UAV flight times, which are crucial for maintaining long-term coverage during extended disaster recovery efforts. Finally, future studies could focus on advanced ML algorithms to improve UAV adaptability, real-time decision-making, security aspects, and interference control in complex environments with different channel conditions.

AUTHOR CONTRIBUTIONS

Nooshin Boroumand Jazi: Conceptualisation; data curation; formal analysis; methodology; software; writing—original draft; writing—review and editing. **Farhad Faghani**: Conceptualisation; formal analysis; investigation; methodology; project administration; supervision; writing—review and editing. **Mahmoud Daneshvar Farzanegan**: Conceptualisation; formal analysis; investigation; methodology; resources; validation; visualisation.

CONFLICT OF INTEREST STATEMENT

The authors declare no conflicts of interest.

DATA AVAILABILITY STATEMENT

Data available on request from the authors.

ORCID

Nooshin Boroumand Jazi https://orcid.org/0000-0002-9171-8602

Farhad Faghani https://orcid.org/0000-0002-7401-1074

REFERENCES

1. Jeauneau, V., Jouanneau, L., Kotenkoff, A.: Path planner methods for UAVs in real environment. IFAC-PapersOnLine 1(22), 292–297 (2018). https://doi.org/10.1016/j.ifacol.2018.11.557
2. Basharat, M., Naeem, M., Anpalagan, A.: Priority-based resource allocation in wireless powered UAV-assisted networks. IET Netw. 11(5), 156–168 (2022). https://doi.org/10.1049/ntw2.12044
3. Han, S.I.: Survey on UAV deployment and trajectory in wireless communication networks: applications and challenges. Information 13(8), 389 (2022). https://doi.org/10.3390/info13080389
4. Jee, A., Prakriya, S.: Performance of energy and spectrally efficient AF relay-aided incremental CDRT NOMA-based IoT network with imperfect SIC for smart cities. IEEE Internet Things J. 10(21), 18766–18781 (2022). https://doi.org/10.1109/jiot.2022.3229102
5. Mozaffari, M., Lin, X., Hayes, S.: Toward 6G with connected sky: UAVs and beyond. IEEE Commun. Mag. 59(12), 74–80 (2021). https://doi.org/10.1109/mcom.005.2100142
6. Alsamhi, S.H., et al.: Computing in the sky: a survey on intelligent ubiquitous computing for uav-assisted 6g networks and industry 4.0/5.0. Drones 6(7), 177 (2022). https://doi.org/10.3390/drones6070177
7. Azari, M.M., et al.: Key technologies and system trade-offs for detection and localization of amateur drones. IEEE Commun. Mag. 56(1), 51–57 (2018). https://doi.org/10.1109/mcom.2017.1700442
8. Dai, H., et al.: How to deploy multiple UAVs for providing communication service in an unknown region? IEEE Wireless Communications Letters 8(4), 1276–1279 (2019). https://doi.org/10.1109/lwc.2019.2915296
9. Hu, J., Zhang, H., Song, L.: Reinforcement learning for decentralized trajectory design in cellular UAV networks with sense-and-send protocol. IEEE Internet Things J. 6(4), 6177–6189 (2018). https://doi.org/10.1109/jiot.2018.2876513
10. Chen, Y., et al.: A 3D placement of unmanned aerial vehicle base station based on multi-population genetic algorithm for maximizing users with different QoS requirements. In: 2018 IEEE 18th International Conference on Communication Technology (ICCT), pp. 967–972. IEEE (2018)
11. Plachy, J., et al.: Joint positioning of flying base stations and association of users: evolutionary-based approach. IEEE Access 7, 11454–11463 (2019). https://doi.org/10.1109/access.2019.2892564
12. Garg, A.: Machine learning coupled trajectory and communication design for UAV-facilitated wireless networks. arXiv preprint arXiv:2101.10454 (2020)
13. Hydher, H., et al.: Intelligent UAV deployment for a disaster-resilient wireless network. Sensors 20(21), 6140 (2020). https://doi.org/10.3390/s20216140
14. Qu, H., et al.: Rapid deployment of UAVs based on bandwidth resources in emergency scenarios. In: 2020 Information Communication Technologies Conference (ICTC), vol. 29, pp. 86–90. IEEE (2020). https://doi.org/10.1109/ictc49638.2020.9123274
15. Moon, I., Dung, L.T., Kim, T.: Optimal 3D placement of UAV-BS for maximum coverage subject to user priorities and distributions. Electronics 11(7), 1036 (2022). https://doi.org/10.3390/electronics11071036
16. Kaleem, Z., et al.: Learning-aided UAV 3D placement and power allocation for sum-capacity enhancement under varying altitudes. IEEE Commun. Lett. 26(7), 1633–1637 (2022). https://doi.org/10.1109/lcomm.2022.3172171
17. Mahmood, A., et al.: Joint optimization of 3D placement and radio resource allocation for per-UAV sum rate maximization. IEEE Trans. Veh. Technol. 72(10), 13094–13105 (2023). https://doi.org/10.1109/tvt.2023.3274815
18. Abu-Baker, A., et al.: Efficient data collection in UAV-assisted cluster-based wireless sensor networks for 3D environment: optimization study. J. Sens. 2023(1), 9513868 (2023). https://doi.org/10.1155/2023/9513868
19. Carvajal-Rodríguez, J., et al.: 3D placement optimization in UAV-enabled communications: a systematic mapping study. IEEE Open Journal of Vehicular Technology 5, 523–559 (2024). https://doi.org/10.1109/ojvt.2024.3379751
20. Nguyen, T.M., Ajib, W., Assi, C.: A novel cooperative NOMA for designing UAV-assisted wireless backhaul networks. IEEE J. Sel. Area. Commun. 36(11), 2497–2507 (2018). https://doi.org/10.1109/jsac.2018.2874136
21. Al-Hourani, A., Kandeepan, S., Lardner, S.: Optimal LAP altitude for maximum coverage. IEEE Wireless Communications Letters 3(6), 569–572 (2014). https://doi.org/10.1109/lwc.2014.2342736

20474962, 2025, 1, Downloaded from https://ietresearch.onlinelibrary.wiley.com/doi/10.1049/ntw2.12143 by Readcube (Labtiva Inc.), Wiley Online Library on [10/03/2025]. See the Terms and Conditions (https://onlinelibrary.wiley.com/terms-and-conditions) on Wiley Online Library for rules of use; OA articles are governed by the applicable Creative Commons License

22. Mozaffari, M., et al.: Unmanned aerial vehicle with underlaid device-to-device communications: performance and tradeoffs. IEEE Trans. Wireless Commun. 15(6), 3949–3963 (2016). https://doi.org/10.1109/twc.2016.2531652
23. Bor-Yaliniz, R.I., El-Keyi, A., Yanikomeroglu, H.: Efficient 3-D placement of an aerial base station in next generation cellular networks. In: 2016 IEEE International Conference on Communications (ICC), vol. 22, pp. 1–5. IEEE (2016). https://doi.org/10.1109/icc.2016.7510820
24. Grau, M.D.: Optimal Deployment of UAV Based Mobile Base Stations in Emergency Scenarios. (Master's thesis). Universitat Politècnica de Catalunya
25. Zhang, C., et al.: Review of clustering technology and its application in coordinating vehicle subsystems. Automotive Innovation 6(1), 89–115 (2023). https://doi.org/10.1007/s42154-022-00205-0
26. Lai, C.C., et al.: Interference-aware deployment for maximizing user satisfaction in multi-UAV wireless networks. IEEE Wireless Communications Letters 12(7), 1189–1193 (2023). https://doi.org/10.1109/lwc.2023.3266011
27. Lai, C.C., Wang, L.C., Han, Z.: Data-driven 3D placement of UAV base stations for arbitrarily distributed crowds. In: 2019 IEEE Global Communications Conference (GLOBECOM), vol. 9, pp. 1–6. IEEE (2019). https://doi.org/10.1109/globecom38437.2019.9014210
28. Arvanitaki, A., Pappas, N.: Modeling of a UAV-based data collection system. In: 2017 IEEE 22nd International Workshop on Computer Aided Modeling and Design of Communication Links and Networks (CAMAD), pp. 1–6. IEEE (2017)
29. Ashari, I.F., et al.: Analysis of elbow, silhouette, Davies-Bouldin, Calinski-Harabasz, and rand-index evaluation on k-means algorithm for classifying flood-affected areas in Jakarta. Journal of Applied Informatics and Computing 7(1), 95–103 (2023)

SUPPORTING INFORMATION

Additional supporting information can be found online in the Supporting Information section at the end of this article.

How to cite this article: Jazi, N.B., Faghani, F., Farzanegan, M.D.: An improved affinity propagation method for maximising system sum rate and minimising interference for 3D multi-UAV placement in disaster area. IET Netw (2025). e12143. https://doi.org/10.1049/ntw2.12143

20474962, 2025, 1, Downloaded from https://ietresearch.onlinelibrary.wiley.com/doi/10.1049/ntw2.12143 by Readcube (Labtiva Inc.), Wiley Online Library on [10/03/2025]. See the Terms and Conditions (https://onlinelibrary.wiley.com/terms-and-conditions) on Wiley Online Library for rules of use; OA articles are governed by the applicable Creative Commons License